Hindawi Publishing Corporation
International Journal of Photoenergy
Volume 2015, Article ID 693463, 13 pages
http://dx.doi.org/10.1155/2015/693463

Research Article

Theoretical and Experimental Optical Evaluation and Comparison of Symmetric 2D CPC and V-Trough Collector for Photovoltaic Applications

Damasen Ikwaba Paul

The Open University of Tanzania, P.O. Box 23409, Dar es Salaam, Tanzania

Correspondence should be addressed to Damasen Ikwaba Paul; paul.ikwaba@out.ac.tz

Received 5 August 2015; Revised 28 October 2015; Accepted 4 November 2015

Academic Editor: Cheuk-Lam Ho

This paper presents theoretical and experimental optical evaluation and comparison of symmetric Compound Parabolic Concentrator (CPC) and V-trough collector. For direct optical properties comparison, both concentrators were deliberately designed to have the same geometrical concentration ratio (1.96), aperture area, absorber area, and maximum concentrator length. The theoretical optical evaluation of the CPC and V-trough collector was carried out using a ray-trace technique while the experimental optical efficiency and solar energy flux distributions were analysed using an isolated cell PV module method. Results by simulation analysis showed that for the CPC, the highest optical efficiency was 95% achieved in the interval range of 0° to $\pm 20^\circ$ whereas the highest outdoor experimental optical efficiency was 94% in the interval range of 0° to $\pm 20^\circ$. For the V-tough collector, the highest optical efficiency for simulation and outdoor experiments was about 96% and 93%, respectively, both in the interval range of 0° to $\pm 5^\circ$. Simulation results also showed that the CPC and V-trough exhibit higher variation in non-illumination intensity distributions over the PV module surface for larger incidence angles than lower incidence angles. On the other hand, the maximum power output for the cells with concentrators varied depending on the location of the cell in the PV module.

1. Introduction

One of the greatest challenges facing the world today is breaking fossil fuel dependence and promoting the development of new and renewable sources of energy that can supplement and, where appropriate, replace the diminishing resources of fossil fuels. Solar energy is clearly one of the most promising prospects to these problems since it is non-pollutant, renewable, and available everywhere in the world although with varying intensity. However, solar electricity has not been utilised as much as it should have been due to low photovoltaic (PV) cell conversion efficiency [1], high cost of PV modules [1] and, until recently, the very low cost of oil and gas. An effective way of improving PV cell efficiency is to increase the light intensity on the PV module by using concentrating systems [2]. Concentrating system also increases solar flux at the PV surface thus reducing the area of photovoltaic material required [2, 3].

Solar concentrators are generally categorized as refractive or reflective [4, 5]. The former can be achieved by lenses whilst the latter is accomplished by using glass mirrors or reflectors. Both refractive and reflective concentrators may be further classified as high-concentrating or low concentrating systems. Although higher concentration ratios result in higher light intensities on the PV cells and a possibility of a lower cost per kWh produced, high initial investments for the high-concentrating systems suggest that low-concentrating systems are a more cost effective solution. Low-concentrating collectors are, in principle, less expensive than high concentrators, as they have no moving parts or solar tracking devices. In addition, manufacturing costs are cheaper because their components are simpler and require low cost in maintenance [6].

Extensive research in the design and testing of solar concentrators has resulted in several different concentrating solar collector designs such as flat planar [7], V-trough

concentrator [8–12], polygon concentrators [13], compound-wedged cylindrical concentrators [14], two-faced conical concentrators [15], trapezoidal groove [15], parabolic trough concentrator [5, 16], central receiver collector [7], fresnel lens concentrator [16], conical concentrator [7], compound elliptical concentrator [7], hyperboloidal concentrator [7], spherical concentrator [4], pyramidical concentrator [7], Compound Parabolic Concentrator (CPC) [9, 17, 18], and multisectional concentrators [11]. However, the CPC has been considered the best static concentrator for solar radiation collection [9, 19, 20]. The advantages of the CPC over other solar concentrating systems include high optical efficiency and being able to collect both diffuse and direct radiations [9]. Nevertheless, the use of the CPC is still limited to specialist applications because of nonuniform illumination [17]. On the other hand, the V-trough collector has been considered as the best collector in terms of more uniform illumination [12].

The performance of the CPC and V-trough collector for PV applications depends, amongst other factors, on the optical efficiency and solar flux distribution along the PV module [20–23]. The former is the ratio of the solar energy absorbed by the PV module to the solar energy incident on the aperture of the concentrator [21] while the later shows the distribution of solar flux across the PV module. The evaluation of optical efficiency of a concentrating system is an important process in the characterisation of concentrators because it is a measure of the quality of the concentrating system [20]. On the other hand, the way in which solar radiation is incident on the surface of a PV module within a concentrator is vital to its performance because nonuniform solar energy flux distribution has a significant negative effect on the electrical performance [2]. Both parameters (optical efficiency and solar flux distribution) depend mainly on the total solar energy incident on the aperture of the collector and the total solar energy reaching the PV module. The energy reaching the PV module depends on the optical properties of various materials involved, the geometry of the collector, and the geometrical perfection of the reflecting surface of the concentrator [23].

Theoretical characterisation of a concentrating system for PV application can be achieved by ray-tracing technique [24–27] while experimental optical efficiency and solar energy flux distribution can be achieved using various experimental methods [2, 17, 24, 27]. This paper presents theoretical optical evaluation and comparison of the CPC and V-trough collector using a ray-trace technique while the experimental optical efficiency and solar energy flux distribution were analysed using an isolated cell PV module method. The paper also compares the maximum power output generated by each PV cell within a CPC and V-trough collector for two incidence angles: 0° and 20°.

2. Materials and Methods

2.1. Designing Parameters of a 2D CPC and V-Trough Collector. In this study two concentrators, symmetric 2-dimensional (2D) CPC and V-trough collector, were considered. For direct comparison, both collectors were deliberately designed to have the same geometrical concentration ratio, aperture area, absorber area, and maximum collector length. The CPC was truncated to reduce its height and to ensure that its geometrical concentration ratio is the same as that of a V-trough collector. Table 1 presents the geometrical properties of the designed symmetric 2D CPC (before and after truncation) and V-trough collector.

2.2. Ray-Trace Simulation Program for Theoretical Optical Evaluation. In order to evaluate theoretical optical performance of a 2D CPC and V-trough collector, ray-trace technique was used to determine the acceptance angle, optical efficiency, optical losses, solar energy flux distribution on the PV surface, and general characteristics of angular acceptance function as well as general optical efficiency. The ray-trace technique employed in this work is called "Eazee ray-trace program" developed by Zacharopoulos [24]. For a given direction and irradiance incidence angle, the ray-trace program simulates the transmission path of a ray from the point it strikes on the aperture cover until it is intercepted by the PV module or exits the concentrator through the aperture. The input to the program is a set of values, which depends upon the properties of the materials involved. The inputs for this analysis were extinction coefficient of the aperture cover material, reflectivity of the reflector, incidence and azimuth angles, type of simulation, refractive indices of the media, and absorptance of the absorber (PV module). Table 2 shows the input parameters that were employed in the program with exception of the incidence and azimuth angles.

For a specific set of inputs, a ray-tracing program randomly chooses the coordinates of the striking point for each ray on the aperture cover and determines the path taken by that ray through the aperture cover to the PV module. During the ray passage, the ray-tracing program calculates (for each ray) the point of intersection and the associated angles of incidence and refraction on the surface in question (aperture cover, reflector surfaces, or PV module). The program also calculates the solar energy absorbed and refracted by the reflector surfaces and the total solar energy absorbed by the PV module. Furthermore, the ray-tracing program calculates the energy flux distribution across the PV module as well as number of ray reflections on the reflector surfaces. The program computes all these values for a sufficient number of initial rays such that the averaged outcome of the rays is a fair representation of the simulated illumination.

For this study, the PV module was assumed to be a perfect absorber of the solar irradiation [28] and the reflector surface was assumed to be specular [17] with a reflectivity equal to that of the employed reflector material ($\rho = 0.91$).

2.3. Experimental Optical Characterisation of a 2D CPC and V-Trough Collector

2.3.1. Solar Energy Flux Distribution along the PV Module and Experimental Optical Efficiency. To determine the solar energy flux distribution along the PV module within the CPC and V-trough collector as well as the experimental optical efficiency, an isolated cell PV module was designed and fabricated as detailed in Paul et al. [2]. The overall dimensions

Table 1: Geometrical dimensions of the 2D CPC and V-trough collector.

Parameter	CPC (before truncation)	CPC (after truncation)	V-trough
Acceptance half-angle (°)	30.0	30.7	21.0
Trough angle (°)	[—]	[—]	10.0
Concentration ratio	2.0	1.96	1.96
Aperture width (mm)	218.0	213.64	213.64
Receiver width (mm)	109.0	109.0	109.0
Receiver length (mm)	109.0	109.0	109.0
Maximum height (mm)	282.4	212.07	296.72
Maximum length (mm)	500.0	500.0	500.0

Table 2: Parameters employed in the ray-trace software.

Parameter	Value
Refractive index of glass (n_g)	1.52
Refractive index of air (n_a)	1.00
Glass extinction coefficients (m^{-1})	4.00
End loss coefficient	0.99
Reflectivity of the reflector (ρ_{ref})	0.91
Absorptance of the PV cells	1.00

of the isolated cells PV module were 118 mm × 109 mm which allowed it to fit exactly at the absorber (exit aperture) area of the CPC and V-trough collector. The isolated cells PV module consisted of 11 monocrystalline silicon BP Solar "Saturn" cells with dimensions of 9 mm × 109 mm each [24].

By using an isolated cell PV module as the absorber of the CPC and V-trough collector and measuring current yields from each of the cells it was possible to determine the amount of solar radiation reaching the PV module and its distribution. In this study, the experimental solar flux distribution along the PV module for each collector (CPC and V-trough) was determined using

$$\text{Energy flux concentraion} = \frac{I_{\text{SC, conc}}}{I_{\text{SC, without}}}, \tag{1}$$

where $I_{\text{SC, without}}$ is the short-circuit current of a PV cell without concentrator and $I_{\text{SC, conc}}$ is the short-circuit current of a PV cell with concentrator.

Since the short-circuit current of a PV module, at a constant temperature, depends only on the absorbed solar radiation, the experimental optical efficiency ($\eta_{\text{opt, exp}}$) of each concentrating system (CPC and V-trough) was calculated from the measurements of the short-circuit currents with concentrator and without concentrator using the following equation [29]:

$$\eta_{\text{opt, exp}} = \frac{E_{\text{PV module}}}{E_{\text{aperture}}}, \tag{2}$$

where $E_{\text{PV module}}$ is the total solar energy on the PV module and E_{aperture} is the incident solar energy on the aperture of a concentrator. The incident solar energy on the aperture of the concentrator is given as

$$E_{\text{aperture}} = G_{\text{aperture}} A_{\text{aperture}}, \tag{3}$$

where G_{aperture} is the incident illumination on the aperture of the concentrator and A_{aperture} is the aperture area of the concentrator calculated from

$$A_{\text{aperture}} = A_{\text{PV module}} C_g = L_{\text{PV}} w_T, \tag{4}$$

where L_{PV} is the length of the PV module and w_T is the aperture width of the concentrator.

Since the PV module had 11 isolated cells, the total solar energy on the PV module ($E_{\text{PV module}}$) was calculated from

$$E_{\text{PV module}} = \sum_{\text{PV cell}=1}^{\text{PV cell}=11} E_{\text{PV cell}}, \tag{5}$$

where $E_{\text{PV cell}}$ was calculated from

$$E_{\text{PV cell}} = \frac{I_{\text{SC, conc}}}{I_{\text{SC, without}}} A_{\text{PV cell}} G_{\text{aperture}}. \tag{6}$$

2.3.2. Experimental Test Procedures. The experimental optical efficiency and solar flux distribution characterisation of the fabricated CPC and V-trough collector were carried out at the roof of the Centre for Sustainable Technologies laboratory building, University of Ulster, UK (56° N, 5° W). The location is influenced by a maritime climate, with highest and lowest solar insolation received at June and December solstices, respectively. For this reason, the experiments were carried out during June and August. To avoid interruption of diffuse radiation, all the measurements presented in this work were carried out only on clear sunny days.

During the measurements, the CPC and V-trough collector (each fabricated by aluminium sheet reflector with reflectivity of 0.91) were aligned in the East-West direction (Figure 1). A special "inclinometer" was used to ensure that the solar vector remained in the meridian plane of the concentrator for the duration of the measurements and also allowed tilt adjustment to achieve the required incidence angle of solar radiation. To minimise alignment errors due to the "movement" of the sun in the sky, the concentrator tilt angle and incidence angle of solar radiation were monitored and adjusted at 5-minute intervals.

The intensity of the solar radiation on the aperture of each concentrator was measured using Kipp and Zonen pyranometer (see Figure 1) while Keithley 2430 SourceMeter was used to produce the I-V curves of each cell for each

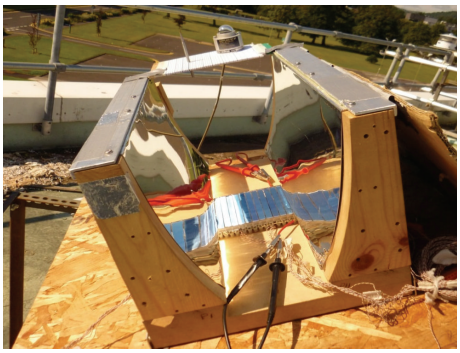

Figure 1: Experimental setup of the CPC at 10° incidence angle for outdoors testing.

experimental test. To determine the variation of the outdoor experimental optical efficiency and solar flux distribution, each test unit (CPC and V-trough) was tilted manually to different incidence angles between 0° and 20°. For a given incidence angle of solar radiation, the isolated cell PV module was placed on the aperture of the concentrator under the incident light. With this setup, the I-V curve of each cell in the PV module was measured and the corresponding short-circuit currents ($I_{\mathrm{SC,\,without}}$) were determined. The module was then placed at the receiver location of the test unit (CPC or V-trough collector) and the I-V measurement for each cell was generated. The short-circuit currents ($I_{\mathrm{SC,\,conc}}$) under the concentrated light were determined for each cell from the corresponding I-V curves. The short-circuit currents were normalised as the measured solar irradiance between each experiment varied slightly.

The experimental solar flux distribution along the PV cell, for both collectors (CPC and V-trough), was examined for 0°, 10°, 15°, and 20° incidence angles using the short-circuit current method.

During incidence angles adjustment, each test unit (PV module at the aperture of a concentrator, CPC or V-trough collector) was covered to avoid overheating of the PV module. Furthermore, an air-fan was used to produce forced cooling and achieve uniform temperature across the PV module during the experimental test.

3. Results and Discussions

3.1. Theoretical Optical Evaluation and Comparison for the CPC and V-Trough Collector

3.1.1. Introduction. The way in which solar radiation is incident on the aperture of a PV concentrator is vital to the performance of a PV module. This is due to the fact that the position in which the rays strike the PV module directly or indirectly (after reflections) is primarily dependent on the incidence angle of the ray, θ_{in} [30, 31]. For this reason, the angular acceptance function, optical efficiency, optical losses, and solar energy flux distributions along the PV module in the CPC and V-trough collector were analysed for 0°, 5°, 10°, 25°, and 27.5° incidence angles.

3.1.2. Optical Analysis for Solar Radiation Incident Perpendicular to the Concentrator Aperture

(1) Ray-Trace Diagrams. In solar concentrating system with a flat receiver, the point to which the ray is finally reflected on the receiver is dependent on two parameters: the angle of incidence of the ray and the geometry of the reflecting surface of the concentrator [31]. The effect of concentrator reflector surface geometry on ray distribution is illustrated in Figure 2, where 50 rays, spaced equally across the apertures of the CPC and V-trough, were traced for solar radiation incident perpendicular to the apertures of the concentrators. It can be seen that all rays reach the PV module in both concentrators either directly or indirectly (after being reflected from the reflector surfaces). However, due to difference in reflecting surfaces profile, the number of rays reaching the receiver directly or after reflection(s) varies between the two concentrators. For example, as shown in Figure 3, while 52% of all incident rays strike the receiver directly in both concentrators, 44% and 48% reach the receiver after one reflection in the CPC and V-trough collector, respectively. The rays which intersect the receiver after two reflections in the CPC were only 2% while none was reflected twice in the V-trough collector.

(2) Angular Acceptance Function and Optical Efficiency. In concentrating systems, the angular acceptance function and optical efficiency depend on the properties (i.e., reflectivity, absorptance, extinction coefficient, and thickness) of the aperture cover material, reflectivity of the reflector, and reflector surface geometry [20]. Since both concentrators (CPC and V-trough) were simulated with the same values of the aperture cover glass extinction coefficient, reflectivity, and absorptance, the difference in their angular acceptance function, optical efficiency, and optical losses was a result of the difference in reflecting surface geometry only. This is due to the fact that different reflecting surface geometry profiles have a different number of reflections owing to difference in ray path-length [32]. Therefore, comparisons of angular acceptance function, optical efficiency, and optical losses for the CPC and V-trough concentrators were based on reflecting surface geometry as shown in Figure 4. It can be seen that all incident rays were accepted by both concentrators because they are within the acceptance angle limits. It is observed that both concentrators have high optical efficiency (94% for the CPC and 95% for the V-trough) as a result of most rays reaching the PV module directly or after only one reflection and hence low optical losses by absorption.

(3) Solar Energy Flux Distributions along the PV Module. Although the CPC and V-trough collector had the same concentration ratio and all the rays were intercepted by the PV module as illustrated in Figure 2, the position on which each ray strikes the PV module after reflection(s) was different for each concentrator due to difference in reflecting surface geometry. This is illustrated in Figure 5, where 10,000 rays, equally spaced over the aperture of each concentrator, were traced to examine the effect of reflector surface geometry on the solar energy flux distributions on

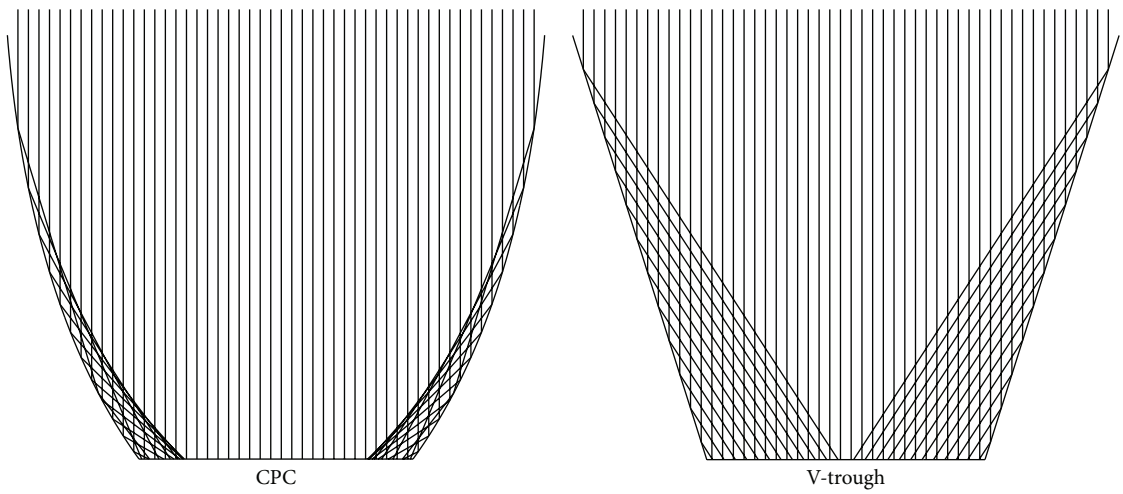

Figure 2: Ray-trace diagrams for the CPC and V-trough collector with solar radiation incident perpendicular to the aperture of the concentrators.

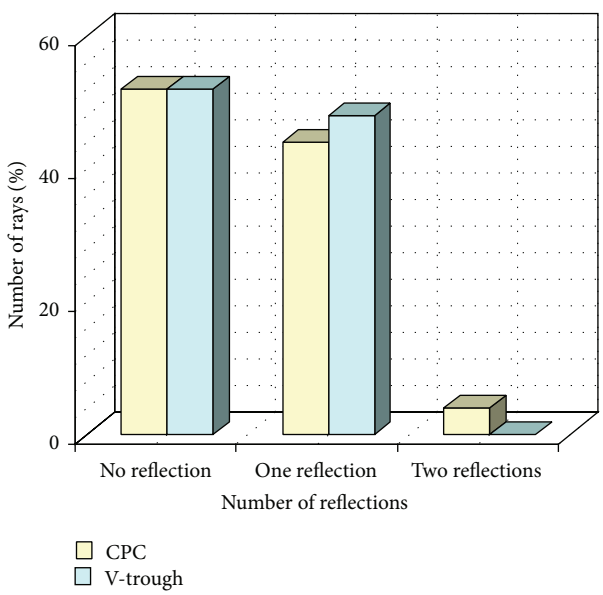

Figure 3: Comparison of number of rays reaching the PV module directly or after reflection(s) for the CPC and V-trough collector when solar radiation incident was perpendicular to the aperture of the concentrators.

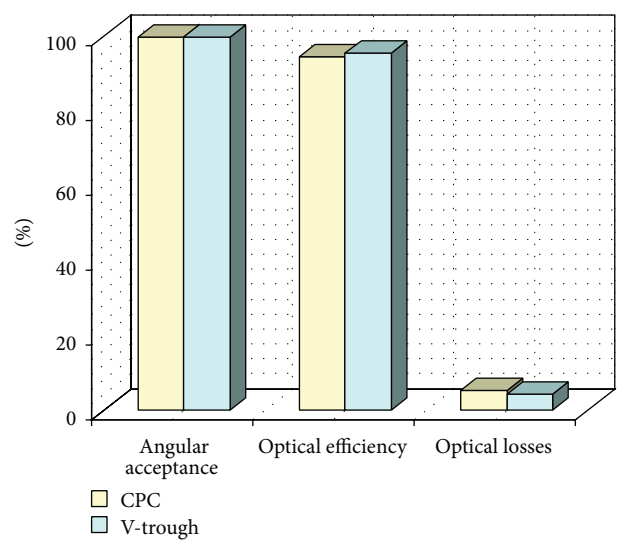

Figure 4: Comparisons of angular acceptance, optical efficiency, and optical losses for the CPC and V-trough collector when solar radiation was incident perpendicular to the aperture of each concentrator.

the PV module. As expected from the ray-trace diagram (Figure 2), the CPC has a high flux concentration at the edges of the PV module because, after reflection, the majority of the rays are concentrated at the edges of the PV module. Figure 5 also shows that the CPC has uniform solar flux distribution between 20 mm and 90 mm since all rays reach the PV module without reflection. On the other hand, the V-trough collector has uniform solar flux distribution over the whole surface of the PV module, except at the centre. The V-trough exhibits nonuniform radiation profile at the centre due to overlapping of rays from the reflector surfaces (see Figure 2). Uniform distribution in V-trough collectors is a function of trough angle [12]. As the trough angle increases, the overall solar energy flux becomes more uniform but the acceptance angle decreases and this reduces the number of rays to be accepted by the concentrator.

Since nonuniform flux distribution on a PV module in which cells are connected in series has significant negative effect on the electrical performance, thus the high solar flux at the edges of the PV module within the CPC (which is about 9 times than the least-illuminated area) will not contribute to an increase in power output. The reason is that when a PV module in which cells are connected in series is nonuniformly illuminated the current generated by the whole PV module is limited by the least-illuminated cell(s) [2]. On the other

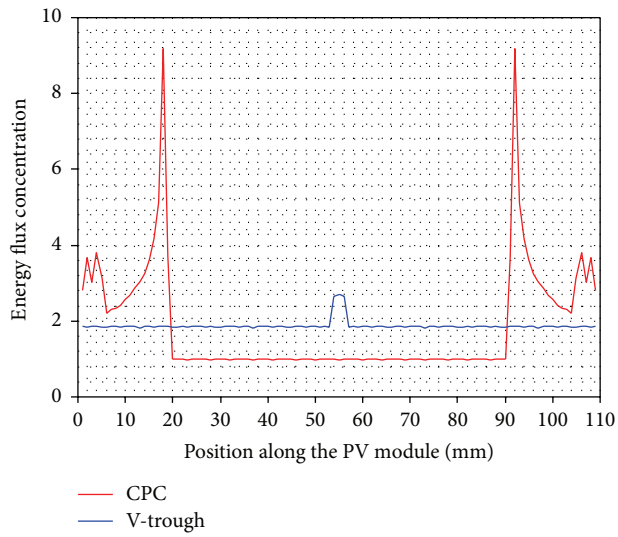

Figure 5: Solar energy flux distributions along the PV module for the CPC and V-trough collector for solar radiation incident perpendicular to the aperture of each concentrator.

hand, the highly concentrated cells located between 50 mm and 60 mm will not contribute to power output when the PV module is used in the V-trough collector as the solar flux in this area is also above the least-illuminated cells. Therefore, if uniform illumination is taken as the only criteria in selecting the best concentrating system for PV application, then it could be economically advantageous to use the V-trough collector as it has more uniform area than the CPC. However, if the PV module consists of isolated cells, the effect of nonuniform illumination results in a power output increase for cells located in the high insolation areas as the current is no longer limited by the least-illuminated cells [2]. In this way, the PV module operates efficiently for the reason that each cell performs to its potential.

3.1.3. Optical Analysis at 5° and 10° Incidence Angles

(1) Ray-Trace Diagrams. Ray-trace diagrams for the CPC and V-trough collector with incident solar radiation at 5° and 10° from the perpendicular to the aperture of each concentrator are shown in Figures 6 and 7, respectively. In both figures, 50 rays, equally spaced over the aperture of each concentrator, were traced to investigate the relationship between incidence angle and concentrator reflecting surface geometry. It can be seen that the number of rays reaching the left and right reflector surfaces before being reflected to the PV module varies with both incidence angle and concentrator reflector surface geometry. At 5°, the numbers of rays reaching the left reflector surface of the CPC and V-trough were 32% and 36%, while those reaching the right reflector surfaces were 16% and 12%, respectively. In both concentrators, increasing the incidence angle from 5° to 10° leads to more rays being reflected onto the PV module by the left reflector surface compared to right reflector (as illustrated in Figure 8, where 42% and 48% reach the left reflector for the CPC and V-trough, resp.).

(2) Angular Acceptance Function and Optical Efficiency. The variation of angular acceptance function, optical efficiency, and optical losses for the CPC and V-trough collector at two different incidence angles (5° and 10°) is shown in Figure 8. It can be seen that, in spite of the difference in surface geometries between the CPC and V-trough, the angular acceptance function is the same (100%) for both concentrators as the incident angle is within the acceptance limits of the concentrator. In addition, both concentrators have a high and similar optical efficiency of about 95% because most of the rays reach the receiver either directly or after one reflection and hence low optical losses as illustrated in Figure 8.

From Figure 8, it can be observed that an increase in incidence angle from 5° to 10° has no significant effect in the angular acceptance function in both concentrators because all the incidence rays still reach the PV module. It is also observed in Figure 8 that an increase in incidence angle has no significant effect on the optical efficiency and optical losses of both concentrators because, as indicated in Table 3, both concentrators had approximately the same number of rays that reach the receiver directly and after one reflection.

(3) Solar Energy Flux Distributions along the PV Module. Figure 9 shows the solar energy flux distributions along the PV module for the CPC and V-trough collector with an incident solar radiation at 5° and 10° from the perpendicular to the aperture of the concentrator. For each angle of incidence, 10,000 rays, equally spaced over the apertures of each collector, were traced. It can be seen that the solar energy flux distribution for each concentrator is nonuniform and the magnitude of illumination uniformity varies with incidence angle and concentrator reflector surface geometry. As illustrated in the figure, the CPC has four illumination intensity peaks; the two highest peaks occur at 20 mm to 28 mm and 97 mm to 106 mm whilst the smallest peaks are found at the edges of the PV module. As the incidence angle increases from 5° to 10°, the highest intensity peak on the left increases in magnitude and shifts to the right whilst the high intensity peak on the right side of the PV module decreases in magnitude and becomes much narrower. It is also noted from Figure 9 that the solar energy flux is distributed uniformly for the CPC between 28 mm and 97 mm when the solar radiation incidence angle is 5°. However, the uniformity in solar energy flux distribution shifts to 38 mm and 101 mm when the incidence angle increases to 10°. The reason for the shift in intensity peaks and uniformity area is due to the fact that at this incidence angle more rays are being reflected from the left reflector and, after reflection, they are focused towards the edge of the right side of the PV module.

For the V-trough collector, it can be seen from Figure 9 that it has only one high solar peak at both incidence angles. However, due to most rays being reflected from the left reflector, the peak shifts towards the edge of the right side of the PV module and becomes much wider as the incidence angle increases to 10°.

The solar energy flux distribution analysis presented in Figure 9 leads to the conclusion that if the PV module used in each concentrator consists of cells in series connection, then

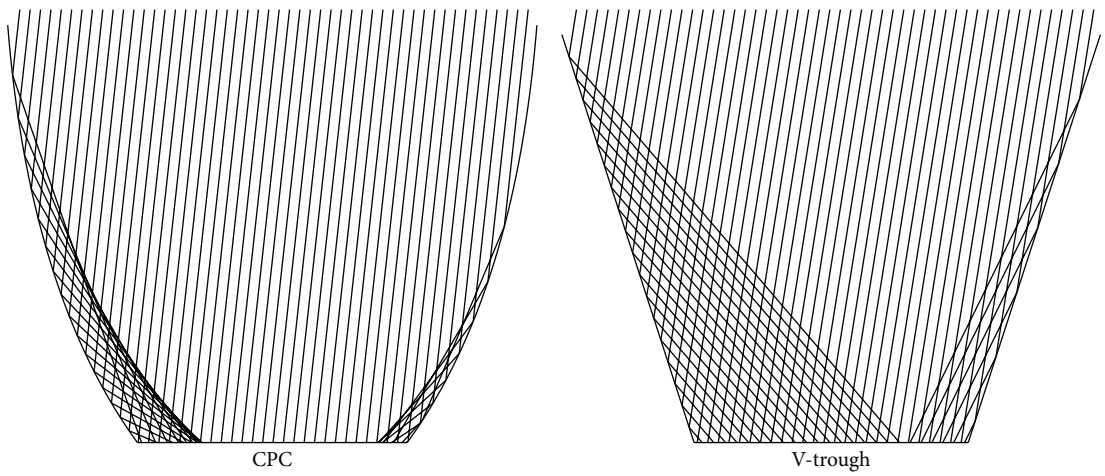

Figure 6: Ray-trace diagrams for the CPC and V-trough collector with solar radiation incident at 5° from the perpendicular to the aperture of each collector.

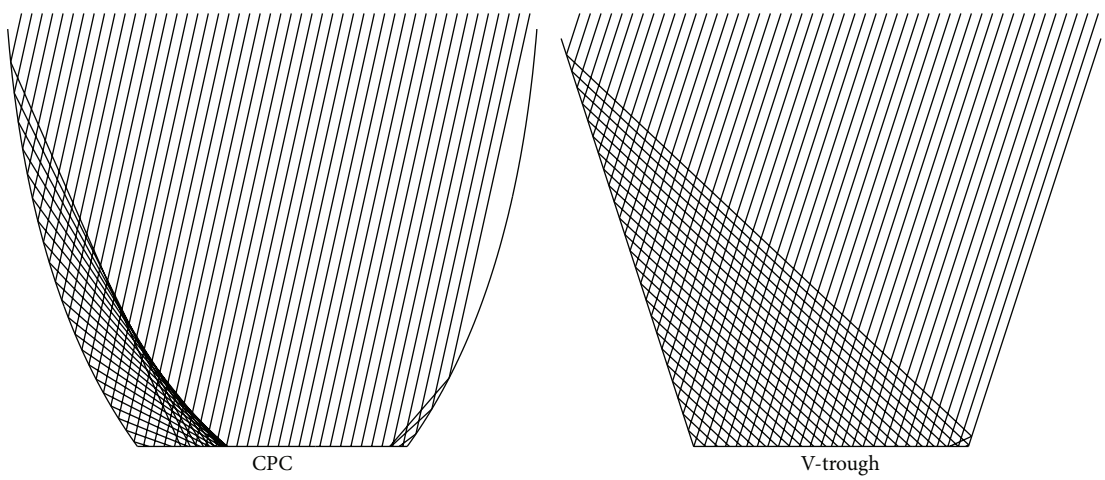

Figure 7: Ray-trace diagrams for the CPC and V-trough collector with solar radiation incident at 10° from the perpendicular to the aperture of each concentrator.

the PV module within the V-trough collector will generate more electrical power output than the PV module with the CPC. The reason is that the values of solar energy flux in the lowest illumination region (which limit the generated current) are higher and more uniform in the V-trough collector than in the CPC. However, if the PV module is made of isolated cells, then the sum of power output from the PV module with the CPC will be greater than a similar module with the V-trough. This is because when sharp peaks of solar radiation flux exist, the absorbed high solar irradiance (by an individual cell) is converted to high current and hence high power output as the photogenerated current is not limited [2].

3.1.4. Optical Analysis at 25° and 27.5° Incidence Angles

(1) Ray-Trace Diagrams. Ray-trace diagrams for the CPC and V-trough collector with incident solar radiation at 25° and 27.5° from the perpendicular to the aperture of the collector are shown in Figures 10 and 11, respectively. It can be seen from Figure 10 that all incident rays reach the PV module for the CPC whilst 20% are rejected in the V-trough collector. The rejected rays in the V-trough are due to incident angle being greater than the acceptance angle of the collector (see Table 1).

Increasing the incidence angle to 27.5° (Figure 11) causes 34% of the rays incident on the V-trough to be rejected and most of the accepted rays are reflected more than two times before intersecting the PV module (see Table 3). These two factors result in a decrease in optical efficiency and increase in optical losses as illustrated in Figure 12. On the other hand, increasing the incidence angle to 27.5° causes the majority of rays to be concentrated near the edge of the right side of the PV module for the CPC collector.

(2) Angular Acceptance Function and Optical Efficiency. The comparison of angular acceptance function, optical efficiency, and optical losses for the CPC and V-trough at two different incidence angles (25° and 27.5°) is given in

Table 3: Variations in ray reflections as a function of incidence angle and concentrator reflecting surface geometry.

Incidence angle (°)	CPC			V-trough		
	No reflection (%)	One reflection (%)	Two reflections (%)	No reflection (%)	One reflection (%)	Two or more reflections (%)
0	52	44	4	52	48	0
5	52	46	2	52	48	0
10	52	48	0	52	44	2
25	28	72	0	10	40	40
27.5	24	76	0	2	40	58

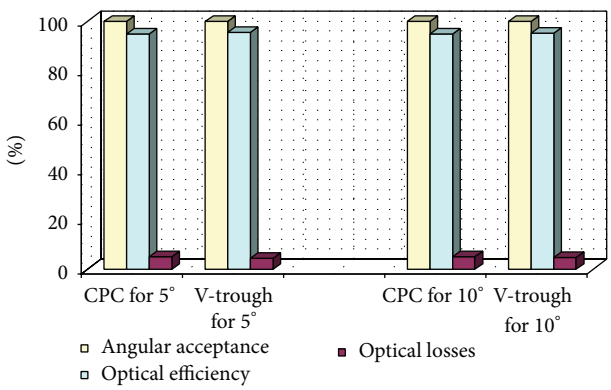

Figure 8: Comparisons of angular acceptance, optical efficiency, and optical losses of the CPC and V-trough for solar radiation incident at 5° and 10°.

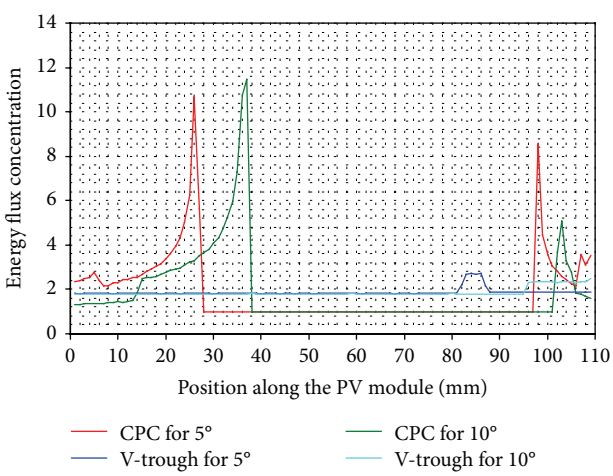

Figure 9: Solar flux distributions along the PV module for the CPC and V-trough collector for solar radiation incident at 5° and 10° from the perpendicular to the aperture of the collector.

Figure 12. Due to difference in reflecting surface geometry, only the CPC attained an angular acceptance of 100% at both incidence angles whilst the V-trough had only 80% at 25°. An increase in incidence angle from 25° to 27.5° decreases significantly the angular acceptance to 54% for the V-trough due to incidence angle being greater than the acceptance angle of the collector.

As shown in Table 3, when the incidence angle is between 25° and 27.5°, the number of rays reaching the PV module directly decreases considerably for each concentrator. This results in higher optical losses and lower optical efficiency as presented in Figure 12. For the V-trough collector, higher optical losses are also due to rays which are rejected.

(3) Solar Energy Flux Distribution along the PV Module. Figure 13 shows the solar energy flux distribution along the PV module for the CPC and V-trough collector with incident angles at 25° and 27.5° from the perpendicular to the aperture of the concentrator. For each angle of incidence, 10,000 rays, equally spaced across the aperture of the collector, were traced. It can be observed from this figure that solar energy flux distribution across the PV module for each concentrator is nonuniform and the magnitude of illumination uniformity varies with incidence angle and type of the concentrator reflector surface geometry. As illustrated in Figure 13, the CPC at 25° has maximum solar energy peak of up to 42 between 80 mm and 87 mm while the magnitude of solar energy flux for the V-trough is very low.

As the incidence angle increases to 27.5°, 59% of all the accepted rays in the CPC are focused onto a very small portion at the edge of the right side of the PV module, giving a peak of solar concentration up to 48 compared with less than 2 for the V-trough collector. Low solar energy peak for the V-trough is due to multiple reflections and rejected rays. Due to high solar energy flux near the edge of the right side of the PV module for the CPC, an increase in local temperature and a significant reduction in conversion efficiency are expected at these incidence angles in real applications.

3.1.5. General Characteristics of Angular Acceptance Function and Optical Efficiency within ±90° Incidence Angles

(1) Angular Acceptance Function. In an East-West alignment, stationary CPC and V-trough collector accept solar radiation in the range of −90° and +90° incidence angle. For this reason, the angular acceptance function and optical efficiency of the two concentrators were also analysed for a full range of incidence angles. Figure 14 shows the variation of angular acceptance as a function of incidence angle for the two collectors. It can be seen that both concentrators have an equal angular acceptance of 100% within their acceptance angle limits. However, due to difference in reflector surface

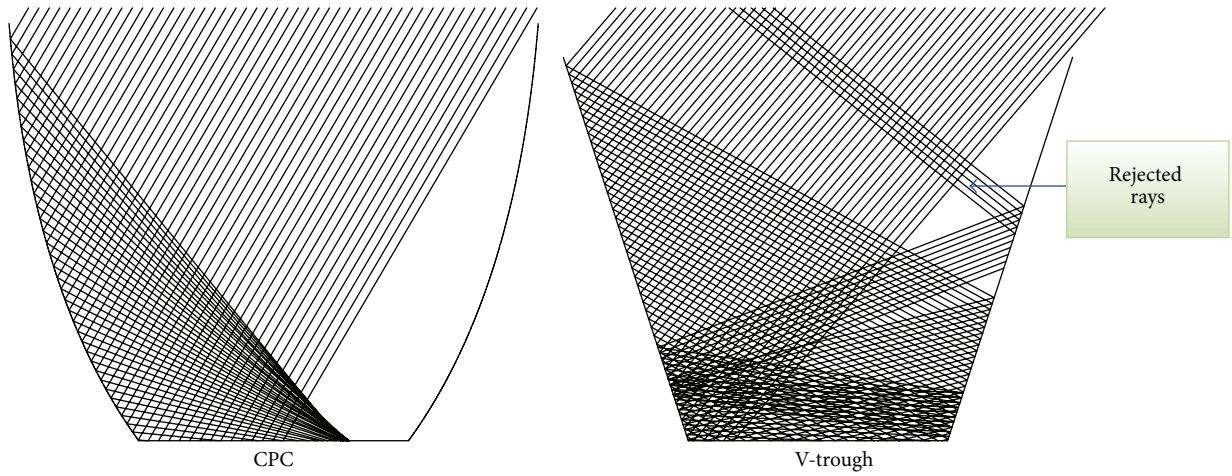

Figure 10: Ray-trace diagrams for the CPC and V-trough collector with solar radiation incident at 25° from the perpendicular to the aperture of the concentrator.

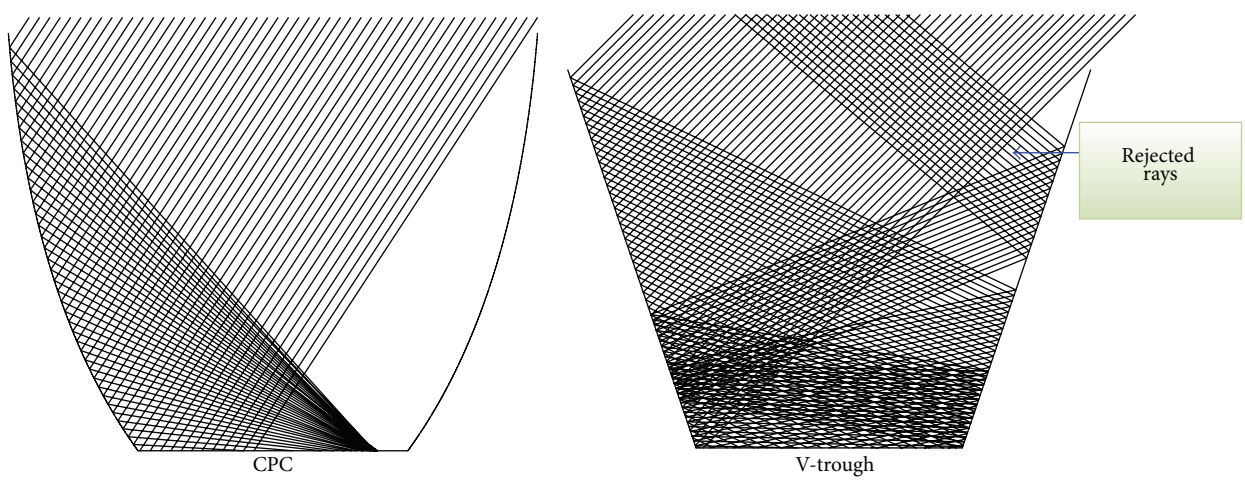

Figure 11: Ray-trace diagrams for the CPC and V-trough collector with solar radiation incident at 27.5° from the perpendicular to the aperture of the concentrator.

geometries, the angular acceptance function of each concentrator changes towards the upper limits of the acceptance angle. It can be observed from Figure 14 that, for the CPC, the angular acceptance increases linearly from 0% at −37.5° to 100% at −27.5° and remains almost constant within ±27.5° incidence angles. It deceases linearly from 100% to 0% in the +27.5° to +37.5° incidence angle range. On the other hand, the angular acceptance function for the V-trough increases linearly from 0% at −42.5° to 100% at −20° and remains constant within ±20° incidence angles. It deceases linearly from 100% to 0% in the +20° to +42.5° incidence angle range.

Although both the CPC and V-trough have equal concentration ratios and aperture areas, they have difference angular acceptance function beyond their acceptance angle limits due to difference in heights and reflector surface geometry. It can be seen from Figure 14 that the V-trough has a higher angular acceptance function than the CPC above ±30°. Whilst no rays can be collected for incidence angles above ±37.5° for the CPC, the V-trough can collect up to ±42.5°.

(2) Optical Efficiency. The predicted optical efficiencies for the CPC and V-trough are shown in Figure 15. It can be seen that the highest optical efficiency for both concentrators is about 95%. Due to larger acceptance angle and low optical losses, the CPC has higher optical efficiency than the V-trough between −30° and +30°. However, beyond ±30° the V-trough has higher optical efficiency due to higher maximum height than the CPC.

3.2. Experimental Optical Efficiency and Solar Energy Flux Distribution along the PV Module

3.2.1. Experimental Optical Efficiency. Figure 16 shows the experimental optical efficiency of the CPC and V-trough as a function of incidence angles. Comparison between the simulated optical efficiencies (Figure 15) and the experimental optical efficiencies (Figure 16) indicates that both results are in good agreement. For the CPC collector, the highest optical efficiency for simulation result was 95% achieved in

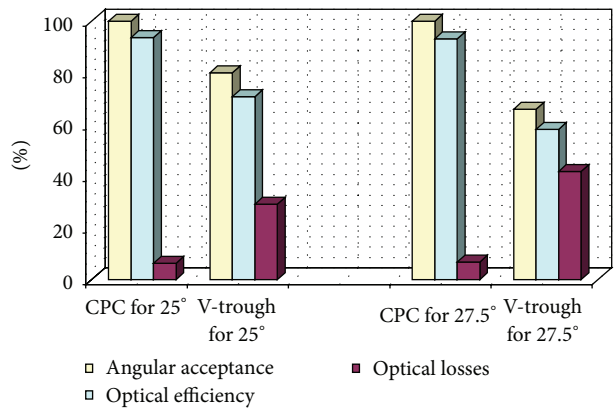

Figure 12: Comparisons of angular acceptance, optical efficiency, and optical losses of the CPC and V-trough for solar radiation incident at 25° and 27.5°.

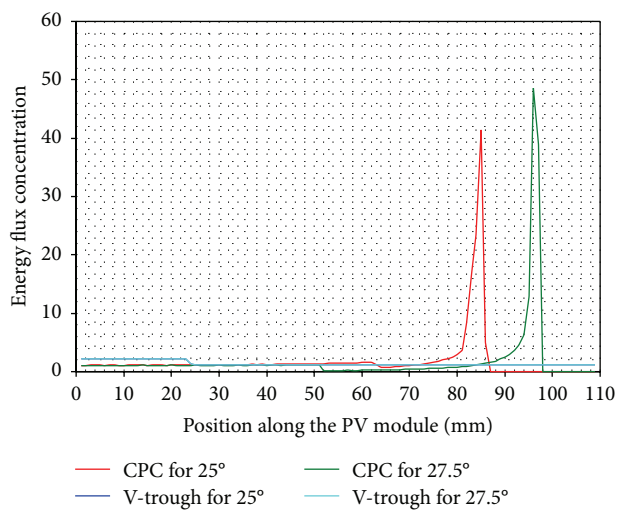

Figure 13: Solar energy flux distributions along the PV module for the CPC and V-trough collector for solar radiation incident at 15° and 20° from the perpendicular to the aperture of the concentrator.

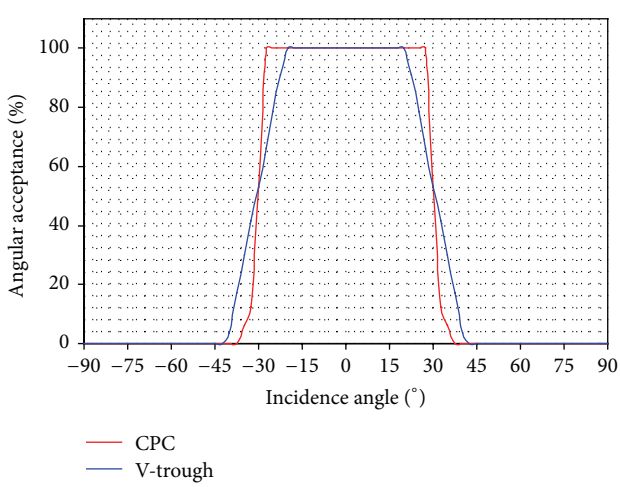

Figure 14: Variations in angular acceptance function with incidence angle for the CPC and V-trough collector.

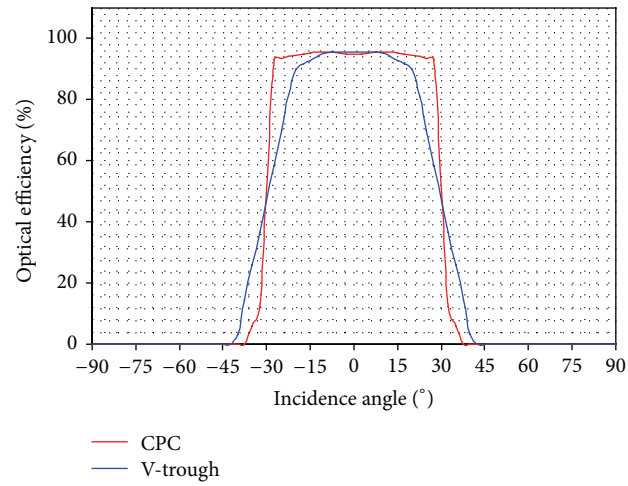

Figure 15: Variation of optical efficiency with incidence angle for the CPC and V-trough collector.

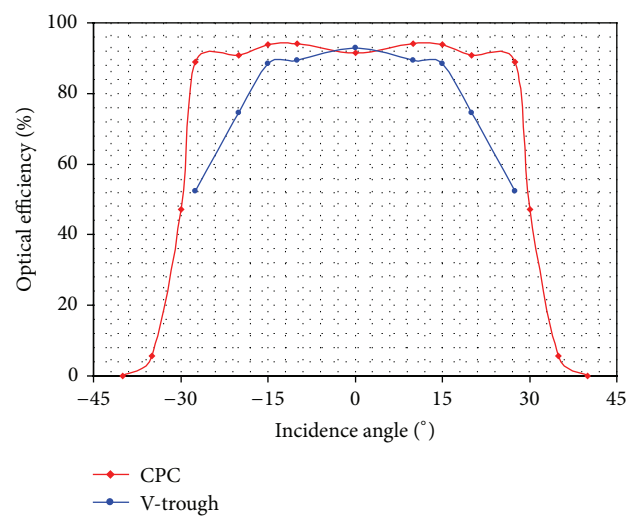

Figure 16: Variation of experimental optical efficiency with incidence angle for the CPC and V-trough collector.

the interval range of 0° to ±20° whereas the highest outdoor experimental optical efficiency was 94% in the interval range of 0° to ±20°. For the V-tough collector, the highest optical efficiency for simulation and outdoor experiments was about 96% and 93%, respectively, both in the interval range of 0° to ±5°. Lower experimental optical efficiencies for the CPC and V-tough were due to resistive losses due to high solar energy flux, solar irradiance reflection losses at the surface of the PV cell, and concentrator fabrication imperfections.

3.2.2. Solar Energy Flux Distribution along the PV Module. Figures 17–20 present the experimentally measured solar energy flux distributions along the PV module for the CPC and V-trough collector for solar radiation incident at 0°, 10°, 15°, and 20°, respectively. As expected from simulation analysis, the energy flux distribution along the PV module for each concentrator (at each incidence angle) is nonuniform

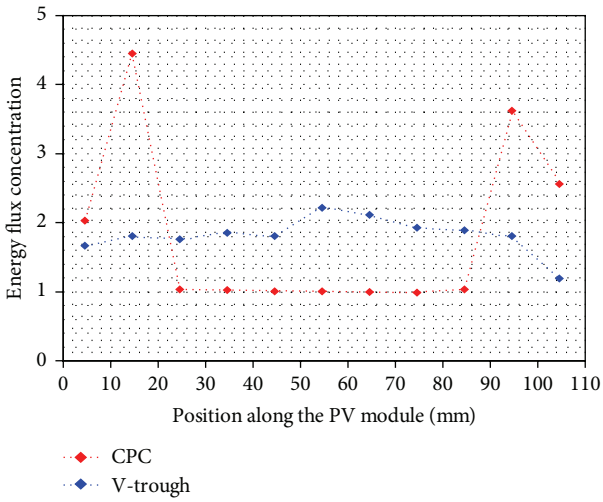

Figure 17: Experimental solar energy flux distributions along the PV module for the CPC and V-trough collector at 0° incidence angle.

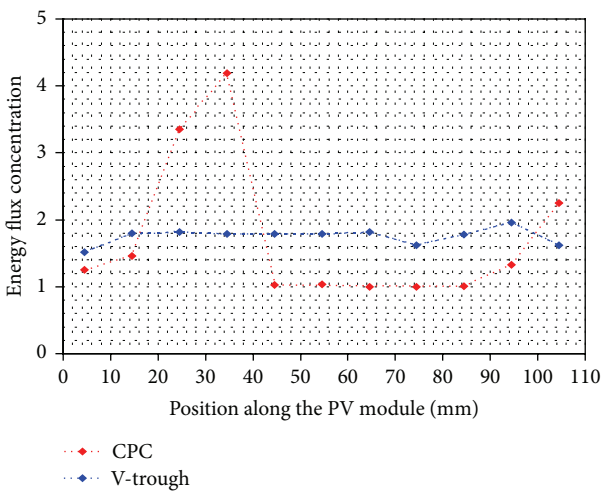

Figure 18: Experimental solar energy flux distributions along the PV module for the CPC and V-trough collector at 10° incidence angle.

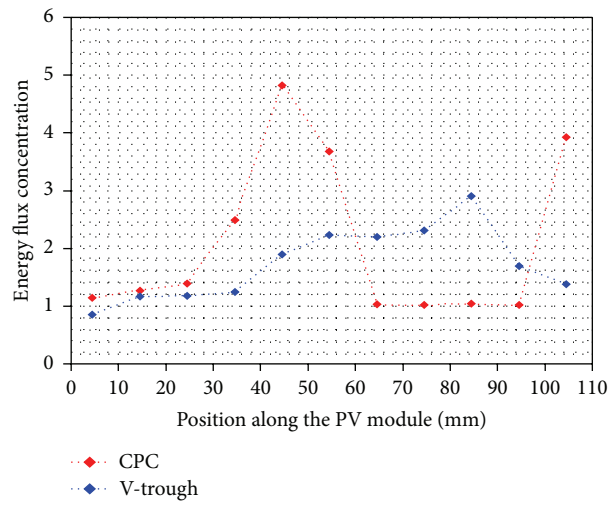

Figure 19: Experimental solar energy flux distributions along the PV module for the CPC and V-trough collector at 15° incidence angle.

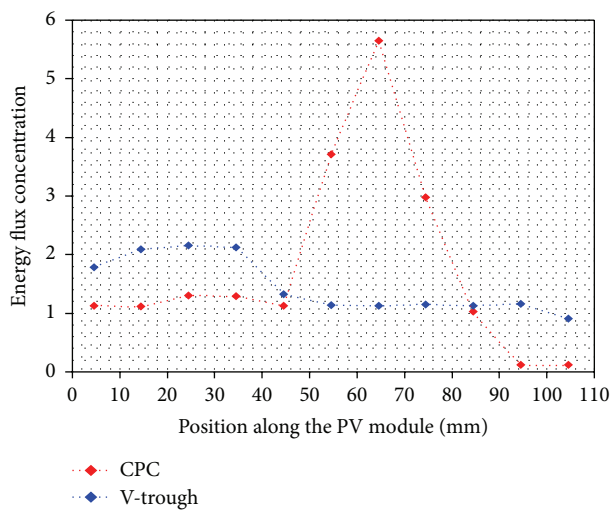

Figure 20: Experimental solar energy flux distributions along the PV module for the CPC and V-trough collector at 20° incidence angle.

and the magnitude of illumination uniformity varies with incidence angle and concentrator reflector surface geometry. For example, from Figure 17 it can be seen that the CPC has a high flux concentration at the edges of the PV module while the V-trough collector has maximum concentration at the centre. However, as the incidence angle increases to 10° (Figure 18), the second highest intensity peak on the CPC which occurs on the right edge of the PV module decreases. The decrease in illumination magnitude is due to the fact that more rays are being reflected from the left CPC reflector and, after reflection, they are focused near the edge of the left side of the PV module.

As shown in Figure 19, when the CPC incidence angle increases to 15°, the highest intensity peak increases in magnitude to 4.8 and shifts to the right side of the PV module. At this incidence angle, the solar energy flux distribution for the V-trough becomes more nonuniform towards the right side of the PV module. The reason for the shift in intensity peaks and areas of uniformity for both concentrators is due to the fact that more solar irradiance is being reflected from the left reflector and, after reflection, they are focused towards the edge of the right side of the PV module. Increasing incidence angle further to 20° (Figure 20) causes all the solar irradiance in the CPC to be incident on the left reflector, as the consequence, high energy concentration area (of about 5.6), is evident near the middle of the PV module. In contrast, the high energy peak for the V-trough decreases in magnitude from 2.0 at 15° to 1.8 at 20°.

From Figures 17-18, a comparison of uniformity distribution between the two concentrators indicates that the V-trough presents a more homogeneous illumination than the CPC.

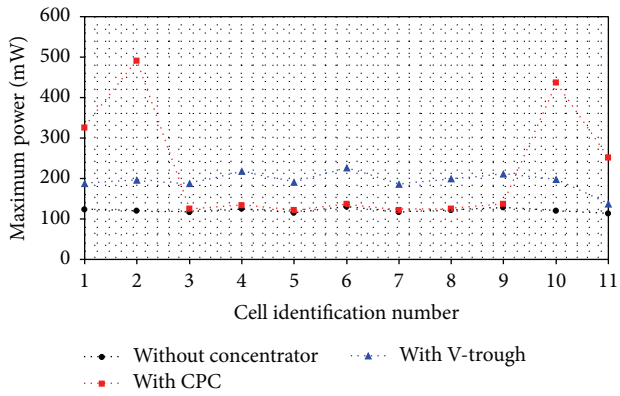

Figure 21: Comparison of maximum power output for cells with and without concentrator when solar radiation incident was perpendicular to the aperture of the test unit.

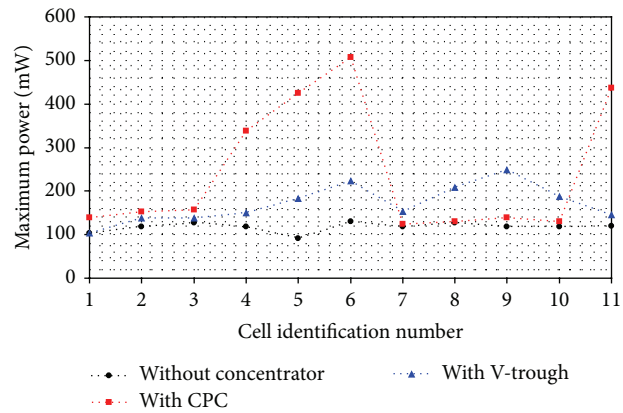

Figure 22: Comparison of maximum power output for cells with and without concentrator when the incident solar irradiance was 20° from perpendicular to the aperture of the test unit.

3.3. Maximum Power Output. To examine the effects of solar radiation incidence angle on the maximum power output of each cell, the PV module with and without concentrator was tilted manually to different incidence angles. However, for the purpose of this paper, only the variations in maximum power output for 0° and 20° incidence angles are presented. For each angle of incidence, a complete I-V curve measurement was recorded for each cell with and without concentrators. From the I-V curve, the maximum power output of each cell under each system was extracted. Figures 21 and 22 show the variations of maximum power output power of each cell for three different cases (without concentrator, with the CPC, and with a V-trough) when the solar radiation was incident at 0° and 20° from the perpendicular to the aperture of the test unit. It can be seen from both figures that the maximum power output for the cells without concentrator was approximately constant as there was no variation in the energy flux received at both incidence angles. However, the maximum power output for the PV cells with the CPC and V-trough collector at both incidence angles varied with the energy flux received by each cell. In other words, the maximum power output follows similar profiles as the experimental solar radiation flux distributions on each cell (see Figures 17 and 20). For the CPC at 0° incidence angle, the maximum power output varied from 120 mW (for cell number 7 in the least illumination region) to about 500 mW (for cell number 2 in the peak energy flux area). On the other hand, the maximum power output for cells within the V-trough varied from 135 mW (for cell number 11 in the least illumination region) to about 225 mW (for cell number 6 in the peak energy flux region).

As the solar radiation incident angle increases to 20°, the highest power output (of about 500 mW) for the PV cells within the CPC was recorded at cell number 4 while the lowest power output of about 100 mW was measured at cell number 10. However, due to difference in reflecting surface geometry between the CPC and V-trough collector as well as the optical efficiency, the highest power output for the PV cells with a V-trough collector was about 250 mW at cell number 9 whereas the lowest power output of about 100 mW was recorded at cell number 1.

4. Conclusions

In this work, a detailed simulation optical analysis, experimental optical efficiency, and solar energy flux distribution along the PV module as well as the maximum power output with the CPC and V-trough collector have been presented. Results by simulation analysis showed that, in spite of both concentrators having the same concentration ratio and aperture area, the concentrators had different optical behaviour, except for the angular acceptance in the interval $-20^\circ \leq \theta_{in} \leq 20^\circ$ and optical efficiency in the interval $-10^\circ \leq \theta_{in} \leq 10^\circ$. For the CPC, the highest optical efficiency for simulation result was 95% achieved in the interval range of 0° to ±20° whereas the highest outdoor experimental optical efficiency was 94% in the interval range of 0° to ±20°. For the V-tough collector, the highest optical efficiency for simulation and outdoor experiments was about 96% and 93%, respectively, both in the interval range of 0° to ±5°.

Theoretical results indicated that the CPC and V-trough exhibit higher variations in non-illumination intensity distributions over the PV module surface for larger incidence angles. On the other hand, the maximum power output for the cells with concentrators varied depending on the location of the cell in the PV module as well as the reflecting surface geometry of a concentrator.

Conflict of Interests

The author declares that there is no conflict of interests regarding the publication of this paper.

References

[1] H. Baig, N. Sarmah, D. Chemisana, J. Rosell, and T. K. Mallick, "Enhancing performance of a linear dielectric based concentrating photovoltaic system using a reflective film along the edge," *Energy*, vol. 73, pp. 177–191, 2014.

[2] D. I. Paul, M. Smyth, A. Zacharopoulos, and J. Mondol, "The design, fabrication and indoor experimental characterisation of an isolated cell photovoltaic module," *Solar Energy*, vol. 88, pp. 1–12, 2013.

[3] B. Norton, P. C. Eames, T. K. Mallick et al., "Enhancing the performance of building integrated photovoltaics," *Solar Energy*, vol. 85, no. 8, pp. 1629–1664, 2011.

[4] K. L. Chopra and S. R. Das, *Thin Film Solar Cells*, Plenum Press, New York, NY, USA, 1983.

[5] R. M. Swanson, "Photovoltaic concentrators," in *Handbook of Photovoltaic Science and Engineering*, A. Luque and S. S. Hegedus, Eds., chapter 11, John Wiley and Sons, Chichester, UK, 2003.

[6] S. P. P. Cardona, *Coupling of photocatalytic and biological processes as a contribution to the detoxification of water: Catalytic and technological aspects [Ph.D. thesis]*, Federal Institute of Technology in Lausanne, Lausanne, Switzerland, 2001.

[7] Y. A. Abdel-Hadi, *Development of optical concentrator systems for directly solar pumped laser systems [Ph.D. thesis]*, Technical University of Berlin, Berlin, Germany, 2005.

[8] D. L. Merchant and M. H. Cobble, "Mirror solar panels," *Solar Energy*, vol. 10, no. 3, pp. 150–152, 1966.

[9] A. Rabl, "Comparison of solar concentrators," *Solar Energy*, vol. 18, no. 2, pp. 93–111, 1976.

[10] H. F. Chiam, "Planar concentrators for flat-plate solar collectors," *Solar Energy*, vol. 26, no. 6, pp. 503–509, 1981.

[11] V. M. Andreev, V. A. Grilikhes, and V. D. Rumyantsev, *Photovoltaic Conversion of Concentrated Sunlight*, John Wiley & Sons, London, UK, 1997.

[12] N. Fraidenraich, "Design procedure of V-trough cavities for photovoltaic systems," *Progress in Photovoltaics: Research and Applications*, vol. 6, no. 1, pp. 43–54, 1998.

[13] S. A. Hamadto, "Planar-sectioned solar concentrators 1: polygon reflectors," *Applied Optics*, vol. 23, no. 8, pp. 1279–1283, 1984.

[14] K. D. Mannan and L. S. Cheema, "Compound-wedge cylindrical stationary concentrator," *Solar Energy*, vol. 19, no. 6, pp. 751–754, 1977.

[15] K. D. Mannan and R. B. Bannerot, "Optimal geometries for one- and two-faced symmetric side-wall booster mirrors," *Solar Energy*, vol. 21, no. 5, pp. 385–391, 1978.

[16] R. Leutz and A. Suzuki, *Nonimaging Fresnel Lenses: Design and Performance of Solar Concentrators*, vol. 83 of *Springer Series in Optical Sciences*, Springer, Berlin, Germany, 2001.

[17] W. T. Welford and R. Winston, *The Optics of Non-Imaging Concentrators*, Academic Press, New York, NY, USA, 1978.

[18] R. Winston, J. C. Minano, and P. Benitez, *Non-Imaging Optics*, Elsevier Academic Press, London, UK, 2005.

[19] R. Winston and H. Hinterberger, "Principles of cylindrical concentrators for solar energy," *Solar Energy*, vol. 17, no. 4, pp. 255–258, 1975.

[20] A. Rabl, "Optical and thermal properties of compound parabolic concentrators," *Solar Energy*, vol. 18, no. 6, pp. 497–511, 1976.

[21] M. Smyth, A. Zacharopoulos, P. C. Eames, and B. Norton, "An experimental procedure to determine solar energy flux distributions on the absorber of line-axis compound parabolic concentrators," *Renewable Energy*, vol. 16, no. 1–4, pp. 761–764, 1999.

[22] B. Schiricke, R. Pitz-Paal, E. Lüpfert et al., "Experimental verification of optical modeling of parabolic trough collectors by flux measurement," *Journal of Solar Energy Engineering—Transactions of the ASME*, vol. 131, no. 1, pp. 1–6, 2009.

[23] M. Brogren, P. Nostell, and B. Karlsson, "Optical efficiency of a PV–thermal hybrid CPC module for high latitudes," *Solar Energy*, vol. 69, no. supplement 6, pp. 173–185, 2000.

[24] A. Zacharopoulos, *Optical design modelling and experimental characterisation of line-axis concentrators for solar photovoltaic and thermal applications [Ph.D. thesis]*, University of Ulster, Coleraine, UK, 2001.

[25] M. Adsten, B. Hellström, and B. Karlsson, "Measurement of radiation distribution on the absorber in an asymmetric CPC collector," *Solar Energy*, vol. 76, no. 1–3, pp. 199–206, 2004.

[26] J. S. Coventry, *A solar concentrating photovoltaic/thermal collector [Ph.D. thesis]*, Australian National University, Canberra, Australia, 2004.

[27] S. Hatwaambo, H. Hakansson, J. Nilsson, and B. Karlsson, "Angular characterization of low concentrating PV-CPC using low-cost reflectors," *Solar Energy Materials and Solar Cells*, vol. 92, no. 11, pp. 1347–1351, 2008.

[28] M. A. Green, *Third Generation Photovoltaics: Advanced Solar Energy Conversion*, Springer, Berlin, Germany, 2006.

[29] A. Luque, G. Sala, J. C. Arboiro, T. Bruton, D. Cunningham, and N. Mason, "Some results of the EUCLIDES photovoltaic concentrator prototype," *Progress in Photovoltaics: Research and Applications*, vol. 5, no. 3, pp. 195–212, 1997.

[30] A. Rabl, *Active Solar Collectors and Their Applications*, Oxford University Press, New York, NY, USA, 1985.

[31] H. E. I. Khonkar and A. A. M. Sayigh, "Raytrace for compound parabolic concentrator," *Renewable Energy*, vol. 5, no. 1-4, pp. 376–383, 1994.

[32] M. Collares-Pereira, J. O'Gallagher, and A. Rabl, "Approximations to the CPC—a comment on recent papers by Canning and by Shapiro," *Solar Energy*, vol. 21, no. 3, pp. 245–246, 1978.